

LA-6046-MS
Informal Report

Q3

CIC-14 REPORT COLLECTION
**REPRODUCTION
COPY**

UC- 21
Reporting Date: July 1975
Issued: September 1975

Preheat Effects on Microballoon Laser Fusion Implosions

by

G. S. Fraley

R. J. Mason

LOS ALAMOS NATIONAL LABORATORY
3 9338 00365 1428



los alamos
scientific laboratory
of the University of California
LOS ALAMOS, NEW MEXICO 87545

An Affirmative Action/Equal Opportunity Employer

UNITED STATES
ENERGY RESEARCH AND DEVELOPMENT ADMINISTRATION
CONTRACT W-7405-ENG. 36

In the interest of prompt distribution, this report was not edited by the Technical Information staff.

Printed in the United States of America. Available from
National Technical Information Service
U S Department of Commerce
5285 Port Royal Road
Springfield, VA 22151
Price: Printed Copy \$4.00 Microfiche \$2.25

This report was prepared as an account of work sponsored by the United States Government. Neither the United States nor the United States Energy Research and Development Administration, nor any of their employees, nor any of their contractors, subcontractors, or their employees, makes any warranty, express or implied, or assumes any legal liability or responsibility for the accuracy, completeness, or usefulness of any information, apparatus, product, or process disclosed, or represents that its use would not infringe privately owned rights.

PREHEAT EFFECTS ON MICROBALLOON LASER FUSION IMPLOSIONS

by

G. S. Fraley and R. J. Mason



ABSTRACT

Nonequilibrium hydroburn simulations of early laser-driven compression experiments indicate that low energy photons from the vicinity of the ablation surface are preheating the microballoon-pushers, thereby severely limiting the compressions achieved (similar degradation may result from 1-4% energy deposition by superthermal electrons). This implies an 8- to 27- fold increase in the energy requirements for breakeven, unless radiative preheat can be drastically reduced by, say, the use of composite ablator-pushers.

Theory¹ predicts that shells can be compressed to many times solid density by laser-driven ablative implosions. In an ablative implosion only the exterior of the shell is heated. The shell is shocked, compressed, and driven towards the origin by the reaction force to material streaming off. DT fuel inside the shell can thus be brought to densities and temperatures favoring thermonuclear burn.² When a low level of preheat is introduced, the shocks are weakened, the back-pressure is increased, and the degree of shell and fuel and convergence is reduced. Under extreme preheat, the entire shell is raised to high temperatures and pressures before any shocks can cross. It simply expands at both its surfaces, compressing the fuel within, but only to minimal densities.

Laser fusion experiments have been reported by KMSF,³ Los Alamos,^{4,5} and Livermore,⁵ which have produced x-ray pinhole pictures as proof of compression, and from 10^4 to 10^7 neutrons.^{3,5} In this paper we report the results of calculations which indicate that the phenomenology in these experiments is dominated by radiative and, perhaps, superthermal electron preheat. This suggests that, for breakeven with simple scaled versions of the reported targets and pulse shapes, energies well in

excess of 10 kJ may be required.

Pusher Heating

At least three mechanisms are available to heat the pusher-shell: (a) classical electron thermal conduction, (b) radiative redeposition, and (c) superthermal electron transport. The classical conduction is always present, modified, of course, by flux limitation,⁶ as influenced by anomalous effects from ion and magnetic field fluctuations. If excessive energy is deposited in the thermal electrons during an implosion, i.e., typically more than 1 J/ng, then the classical conduction wave will "burn through" the shell, leading to the expanding pusher behavior. This condition is readily avoided, however, with proper pulse shaping.

Radiative preheat arises from the reabsorption of bremsstrahlung, recombination and line radiation photons produced near the ablation surface, where the plasma electrons are typically from 300 to 500 eV. The thickness of the microballoon walls is comparable to the range of such low energy photons, so that a portion of this radiation is redeposited deep in the shells with significant consequence, as we shall demonstrate.

Superthermal electrons are generated when various thresholds for absorptive instability are

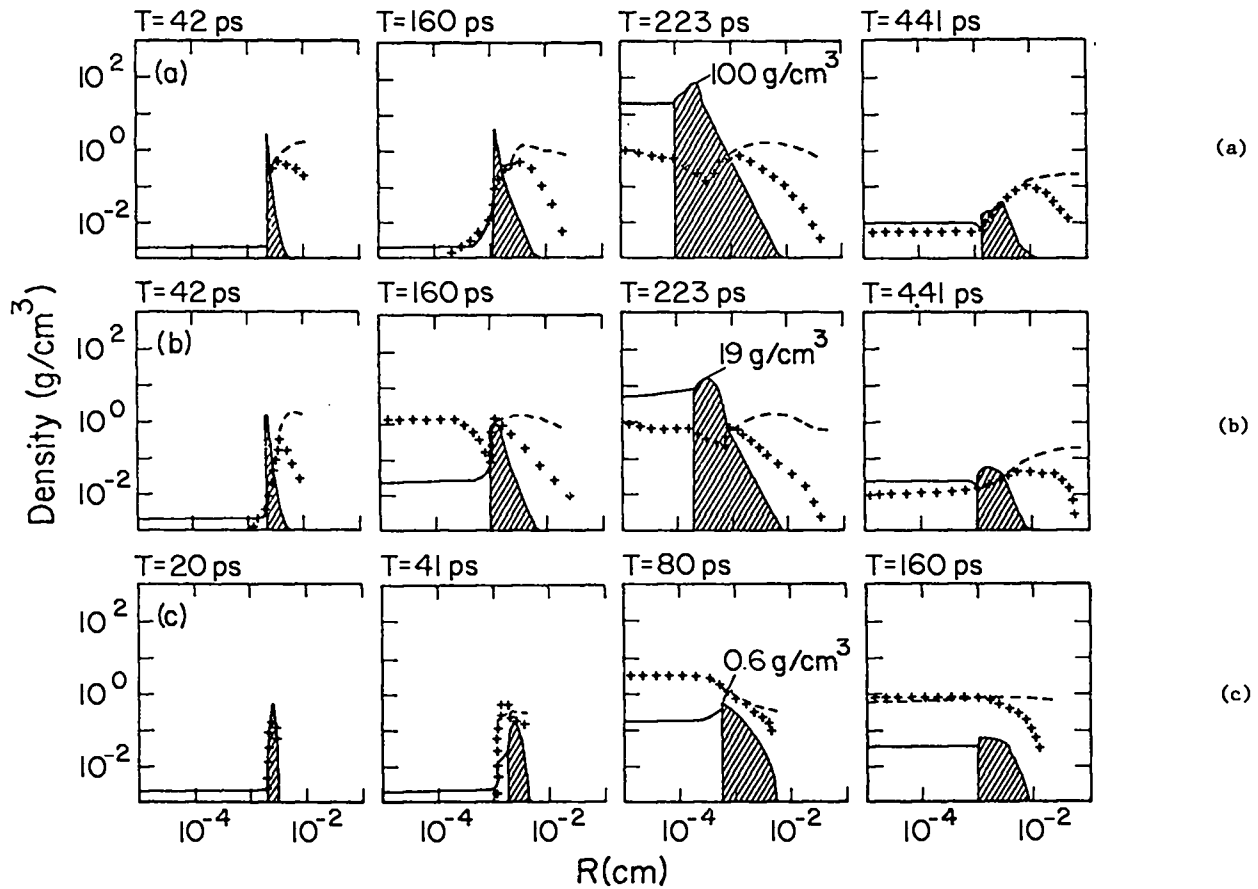


Fig. 1. Implosion of a 52 μm DT-filled microballoon: (a) radiation "off" and no superthermals - pure ablative implosion, (b) radiation "on" and no superthermals - mixed mode implosion, and (c) 100% deposition by superthermals and radiation "on" - pure expanding pusher. ρ - (g/cm^3), T_i ++, T_e -- (keV). Glass is crosshatched.

exceeded. Resonant absorption,⁷ for example, readily furnishes 100 keV electrons at $10^{16} \text{ W}/\text{cm}^2$ 1.06 μm light intensities. At the lower $\sim 10^{15} \text{ W}/\text{cm}^2$ intensities appropriate to the experiments,³⁻⁵ the energy deposited by superthermals still remains an uncertainty.

Microballoon Simulations

Our calculations have been done with the nonequilibrium and 3-T codes described in Ref. 2. Free-bound and line-radiation effects are included in the Monte Carlo, frequency-group nonequilibrium calculations.⁸ The nonequilibrium code has been run with the radiation "on" and "off" (no photons generated)

to probe the radiative preheat dependency. The 3-T calculations diffuse bremsstrahlung in an assumed Planckian by Rosseland mean opacities; they agree generally with the multigroup radiation "off" predictions. In the two codes it is assumed that the superthermal electrons deposit their energy in proportion to the local mass at a constant rate over the length of the pulse. This procedure provides an approximate picture of the effects of long range energy transport by the electrons.

Figure 1 characterizes the general implosion phenomenology that we calculate with the nonequilibrium code for a typical microballoon target shot

TABLE I

PERFORMANCE OF THE 52 μm MICROBALLOON: RADIATIVE AND SUPER-THERMAL PREHEAT

Property	No Rad No Sup	Rad No Sup	Rad 4% Sup	Rad 100% Sup
T_{if}, T_{ef} (keV)	1.0, 0.9	0.7, 0.55	0.7, 0.65	3.7, 1.2
ρ_f (g/cm ³)	21.0	7.0	1.6	0.2
ρ_t (g/cm ³)	100.0	19.0	3.0	0.5
$\langle \rho R \rangle_{tot}$ (g/cm ²)	1.5×10^{-2}	7.0×10^{-3}	2.5×10^{-3}	3.0×10^{-4}
$\langle \rho R \rangle_f$ (g/cm ²)	2.5×10^{-3}	1.2×10^{-3}	4.5×10^{-4}	1.7×10^{-4}
neutrons	5.4×10^6	5.0×10^5	7.0×10^4	8.2×10^7

by KMSF under its contract with ERDA⁹ (shot 110A). The target diameter was 52 μm and the wall thickness was 1.1 μm . The DT (18-13 mix) was at 10 atm. The pulse was square, nominally 240 ps long, and it delivered 4.9 J to the microballoon. Experimentally, 2.5×10^5 neutrons were obtained from this target. Specifics of its calculated performance are recorded in Table I.

The top four frames (a) of Fig. 1 are for the radiation "off" and no superthermals. The implosion is purely ablative. The tamper goes to a maximum density $\rho_t = 100 \text{ g/cm}^3$, when the fuel is at an average density $\rho_f = 21 \text{ g/cm}^3$. The maximum compression of the system, as measured by $\langle \rho R \rangle_{tot} = \int \rho_t dR + \int \rho_f dR$, is $1.5 \times 10^{-2} \text{ g/cm}^2$. The next sequence (b) is for radiation "on" and no superthermals. The preheat drops the maximum tamper density to 19 g/cm^3 and $\langle \rho R \rangle_{tot}$ to $7.0 \times 10^{-3} \text{ g/cm}^2$. The fuel $\langle \rho R \rangle_f = \int \rho_f dR$ is also down by about a factor of two. The predicted number of neutrons drops from 5.4×10^6 to 5.0×10^5 . If we assume that 4% of the energy was delivered in superthermals, the implosion is similar to (b), but ρ_t drops further to 3 g/cm^3 . Finally, with 100% of the deposition through superthermals, we get (c). The tamper drops from its solid value (2.2 g/cm^3) and recompresses at maximum convergence to only 0.6 g/cm^3 . The expanding tamper shock-heats the fuel to 3.7 keV, so that the predicted neutron output rises to 8.2×10^7 . The $\langle \rho R \rangle_f$ obtained in this implosion mode is so low, however, that superthermal ion loss¹⁰ should substantially lower the

actual yield.

Thus, our codes indicate that, in a typical current microballoon experiment, radiative preheat is responsible for a 5-fold reduction in tamper density and a 2-fold reduction in $\langle \rho R \rangle_{tot}$ -- below the values anticipated for a purely ablative implosion. Additional reductions of nearly equal magnitude can derive from a low level of energy deposition by long range superthermal electrons.

Figure 2 plots the 3-T model's predictions for the 52 μm diameter microballoon as a function of the fraction of energy in superthermals, $f_s = \epsilon_s / (\epsilon_s + \epsilon_{th})$; ϵ_{th} is the classical energy deposition in thermal electrons. With 0.1% superthermals we recover $\rho_t = 100 \text{ g/cm}^3$ and $\langle \rho R \rangle_{tot} = 1.5 \times 10^{-2} \text{ g/cm}^2$ (the 3-T code overlooks the line and recombination radiation preheat effects). Only 1% of the energy deposition by superthermals is required for a 3-fold reduction in the peak tamper density.

Mass Scaling and Breakeven

Energy needs scale roughly as the mass m of a given aspect ratio shell. Comparable shell temperatures and collapse velocities are thereby achieved, the shell radii and pulse length then scale as $m^{1/3}$, and the laser intensity at the critical surface becomes mass independent. The 52 μm balloon has a mass of 21 ng. Scaling it up to a 7.5 μg shell requires 1.75 kJ delivered in a 1.7 ns (square) pulse. The bigger shell has a 7.1 μm wall thickness.

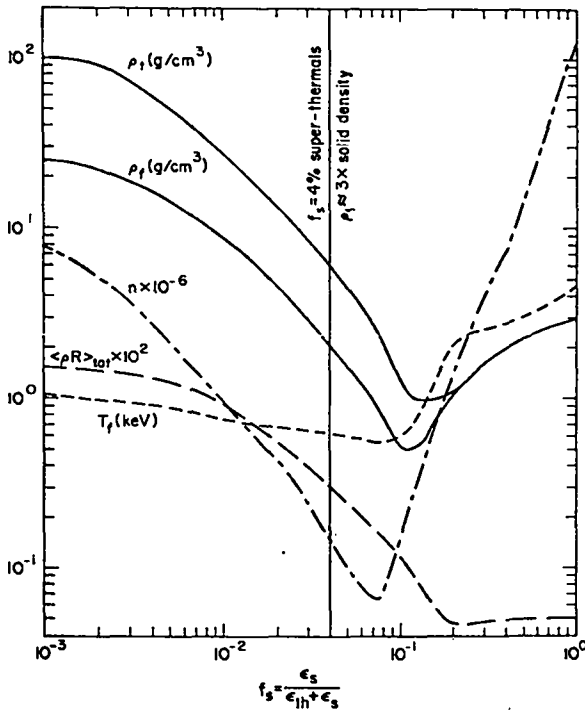


Fig. 2 Implosion characteristics of the 52 μm target as a function of the fractional energy deposition by superthermals f_s .

With the radiation "off" this scaled pellet compresses to $\langle \rho R \rangle_{\text{tot}} = 0.15 \text{ g/cm}^2$; with it "on" $\langle \rho R \rangle_{\text{tot}} = 0.058$. This is a 2.6-fold reduction despite the thicker wall. Scaling further to 428 μg requires 100 kJ of deposition over 6.5 ns. Still, $\langle \rho R \rangle_{\text{tot}}$ drops from 0.62 to 0.34 g/cm^2 and ρ_t goes from 190 g/cm^3 to 50 g/cm^3 , when the multigroup transport is introduced.

The preheat degradation persists beyond the 100 kJ range. We find, however, that replacement of the outer 40% of the glass by a low Z ablator material (Be) can improve the compression substantially (for the 100 kJ pellet $\rho_t = 160 \text{ g/cm}^3$, $\langle \rho R \rangle_{\text{tot}} = 0.52$) by minimizing the output of line and recombination radiation that leads to preheat.

The effective use of pulse shaping and cryogenics will be needed to achieve breakeven at minimal input energies. The DT must be frozen uniformly to the inside of the microballoons, and the shell must resist instabilities under time-tailored laser pulses. Our 3-T calculations indicate¹¹ that breakeven should be possible (ignoring preheat) with 3.5 kJ delivered in a $\epsilon \sim t^3$ pulse over 1.4 ns to a 6.7 μg homogeneous glass microballoon, 470 μm in

diameter, containing a 270 ng DT ice liner. A peak $\langle \rho R \rangle_{\text{tot}}$ of 0.64 g/cm^2 is calculated for this target. If radiative preheat is assumed to cause no greater difficulty than to degrade $\langle \rho R \rangle_{\text{tot}}$ by the 2- to 3-fold factor discussed, then, since $m \sim \langle \rho R \rangle^3$ with fixed shell density, to recover the lost compression we need only scale the pellet mass 8- to 27-fold. Breakeven with no low Z ablator then lies between 28 and 94 kJ. A complication, however, is that in the KMSF-ERDA experiments it appeared that ablation front, Taylor-like instabilities prohibited even linear ramp pulse shaping. This has been attributed to the low transverse thermal conductivity of the glass.⁹

Conclusions and Suggestions

A multigroup photonics treatment is clearly essential for the proper modelling of current and foreseeable laser implosion experiments. We have shown that the breakeven energy needs of microballoon targets will be significantly higher than the optimistic predictions of earlier 3-T calculations unless radiative preheat is markedly reduced. To this end we suggest that an outer fraction of the pusher mass should be converted to low Z material,

e.g., beryllium, to minimize the generation of radiation. This may also stabilize the ablation surface by enhancing the transverse conduction, thus permitting effective pulse shaping. The retention of an inner high Z portion of the pusher has advantages structurally, hydrodynamically,¹¹ and as a super-thermal electron shield.¹² However, for the suppression of flow instabilities, it may be necessary to make the entire pusher out of low Z material.

REFERENCES

1. J. Nuckolls, L. Wood, A. Theissen, and G. Zimmermann, "Laser Compression of Matter to Super-High Densities: Thermonuclear Applications," *Nature (London)* **239**, 139 (1972), J. S. Clarke, H. N. Fisher, and R. J. Mason, "Laser-Driven Implosion of Spherical DT Targets to Thermonuclear Burn Conditions," *Phys. Rev. Lett.* **30**, 89 (1973) and **30**, 249 (1973), K. Brueckner, "Laser Driven Fusion," *IEEE trans on Plasma Sciences PS-1*, **13** (1973).
2. G. S. Fraley, E. J. Linnebur, R. J. Mason and R. L. Morse, "Thermonuclear Burn Characteristics of Compressed Deuterium-Tritium Microspheres," *Phys. Fluids* **17**, 474 (1974), R. J. Mason and R. L. Morse, "Hydrodynamics and Burn of Optimally Imploded Deuterium-Tritium Spheres," *Phys. Fluids* **18**, 816 (1975).
3. G. Charatis et al., "Experimental Study of Laser Heated Spherical Targets," Fifth I.A.E.A. Conference on Plasma Physics and Controlled Thermonuclear Research, Tokyo, Japan, Nov. 11-15, 1974, IAEA-CN-33/fl; P. M. Campbell, G. Charatis, and G. Montry, "Laser-Driven Compression of Glass Microspheres," *Phys. Rev. Lett.* **34**, 74 (1975).
4. G. McCall and R. L. Morse, "Target Compression with One Beam," *Laser Focus* **10**, 40 (December) 1974.
5. G. H. McCall, R. P. Godwin, and D. V. Giovanelli, "Laser Target Interaction Experiments," *IEEE International Conference on Plasma Science*, Ann Arbor, Michigan, May 14-16, 1975, 4A1; and J. F. Holzrichter, H. G. Ahlstrom, E. Storm, and J. Swain, 4A7.
6. R. C. Malone, R. L. McCrory, and R. L. Morse, "Indications of Strongly Flux-Limited Electron Thermal Conduction in Laser-Target Experiments," *Phys. Rev. Lett.* **34**, 721 (1975).
7. D. W. Forslund, J. M. Kindel, K. Lee, E. Lindman, and R. L. Morse, "Theory and Simulation of Resonant Absorption in a Hot Plasma," *Phys. Rev.* **A11**, 679 (1975).
8. G. S. Fraley, "The Integrated Compton Cross Section and Its Use in a Monte Carlo Scheme," Los Alamos Scientific Laboratory report LA-4592 (April 1971).
9. KMS Fusion report U323 (April 12, 1975).
10. D. B. Henderson, "Burn Characteristics of Marginal Deuterium-Tritium Microspheres," *Phys. Rev. Lett.* **33**, 1142 (1974).
11. R. J. Mason, "Performance of Structured Laser Fusion Pellets," (submitted to *Nuclear Fusion*).
12. R. L. Morse and C. W. Nielson, "Occurrence of High Energy Electrons and Surface Expansion in Laser Heated Plasmas," *Phys. Fluids* **16**, 909 (1973), p. 912.